Electronic Supporting Information

Multi-color emission and temperature promoted luminescence efficiency in stimuli-responsive stoichiomorphic ionic co-crystals

Asif A. Malik,[a] Akkarakkaran Thayyil Muhammed Munthasir,[b] Pakkirisamy Thilagar,[b]* and Ajiaz A. Dar[a]*

[a.] *Crystal Engineering Laboratory, Department of Chemistry, University of Kashmir, Hazratbal, Srinagar-190006, Jammu & Kashmir, India.*
[b.] *Department of Inorganic and Physical Chemistry, Indian Institute of Science, Bangalore 560012, India.*
* Corresponding author: thilagar@iisc.ac.in;
aijazku2015@gmail.com/daraijaz@uok.edu.in ORCiD: 0000-0002-6180-274X;

Table S1: Crystallographic Table of **P1** and **P2.**

Compounds	P1	P2
CCDC No.	2420428	2420429
Empirical formula	C34 H28 N4 O6 S2	C34 H28 N4 O7 S2 H_2O
Fw	668.72	502.50
Temp [K]	150 K	293 K
Crystal system	Orthorhombic	Monoclinic
Space group	A b a 2	P 21/c
a, [Å]	13.6097(6)	7.4079(17)
b, [Å]	11.9939(6)	12.821(3)
c, [Å]	18.2054(7)	12.291(3)
α, [°]	90	90
β, [°]	90	105.384(7)
γ, [°]	90	90
V, [Å^3]	2971.7(2)	1125.5(5)
Z	4	2
D(calcd) [Mg/cm^3]	1.495	1.483
μ [mm^{-1}]	0.235	0.289
Θ range [°]	24.975	24.999
Reflns collected	2568	1982
Indep. Reflns	2208	1825
GOF	1.080	1.131
R1(I_0>2σ(I_0)	0.0821	0.0474
wR2(all data)	0.2320	0.1331

^{1}H NMR: To validate the stoichiometry of the synthesized compounds, detailed analysis of the ^{1}H NMR spectra were conducted, as shown in Figures S1 and S2 below.

For compound **P1**, the spectrum clearly supports a 1:2 stoichiometric ratio, as evidenced by the integration of key aromatic and aliphatic proton signals. Specifically, a singlet at ~δ 6.8 ppm corresponding to 1H from the acid component is accompanied by signals at ~δ 7.2–7.8 ppm integrating for 4H and 8H, consistent with the presence of two equivalents of the base component. For **P2**, the spectrum reveals equimolar integration of characteristic aromatic protons (~δ 7.0–7.8 ppm), showing a 4H:4H ratio from the acid and base components, respectively, with matching aliphatic signal integration, confirming a 1:1 stoichiometry.

Note: On dissolution in high polar solvent like DMSo the co-crystals possibly disintegrate, which is accompanied by reversal of proton transfer, therefore unlike in crystal phase the protons on two aromatic rigs of BPe will form equivalent sets in both complexes.

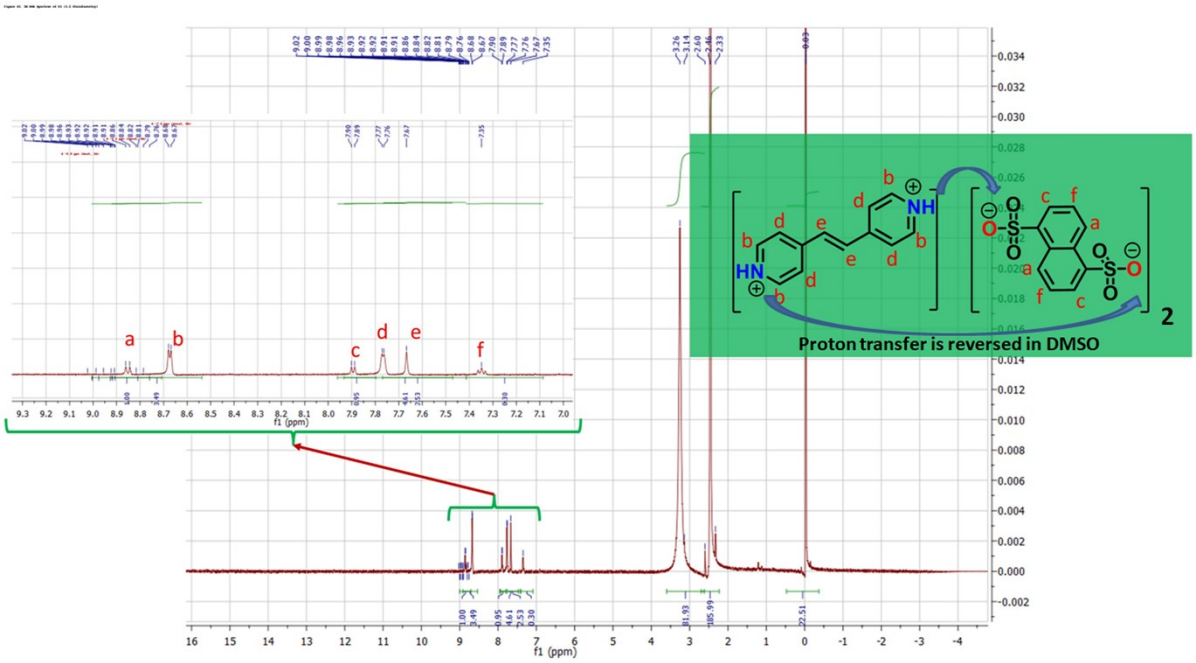

Figure S1: ^{1}H-NMR spectra of **P1** recorded in DMSO-d_6 solvent (500MHz).

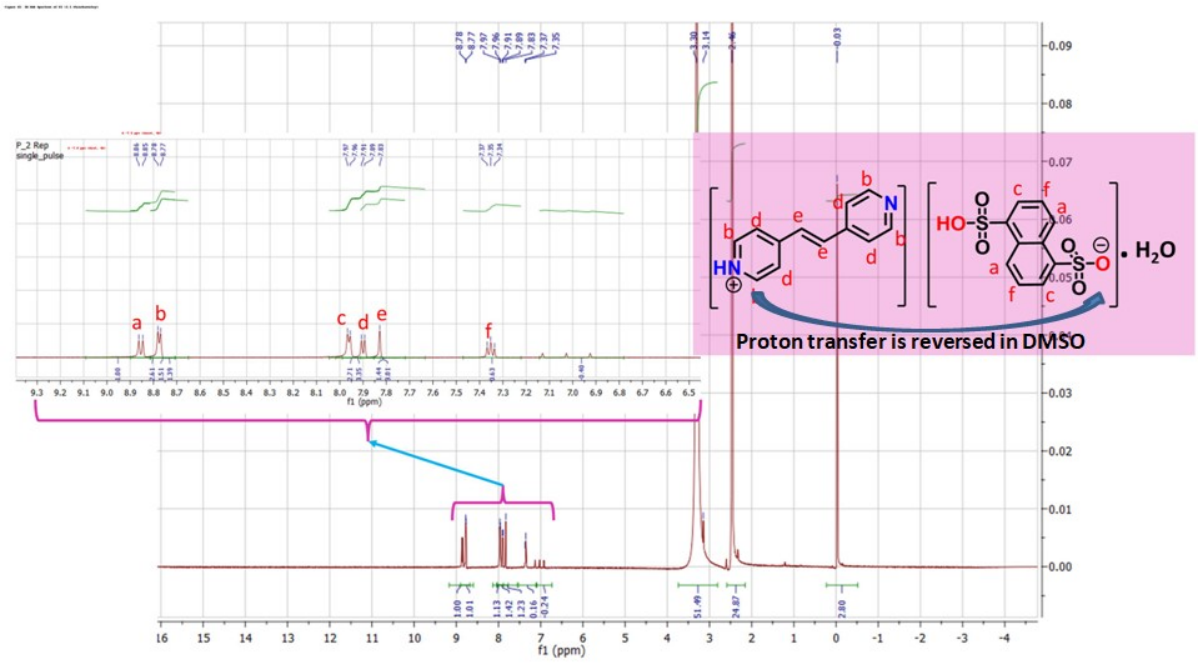

Figure S2: ^{1}H-NMR spectra of **P2** recorded in DMSO-d_6 solvent (500MHz).

^{13}C NMR (500 MHz, DMSO-d_6) δ 146.59 – 146.38 (m), 145.56 – 145.17 (m), 134.91 – 134.52 (m), 133.75 – 133.54 (m), 133.49 – 133.28 (m), 129.25 – 129.04 (m), 127.44 – 127.23 (m), 124.30 – 123.93 (m).

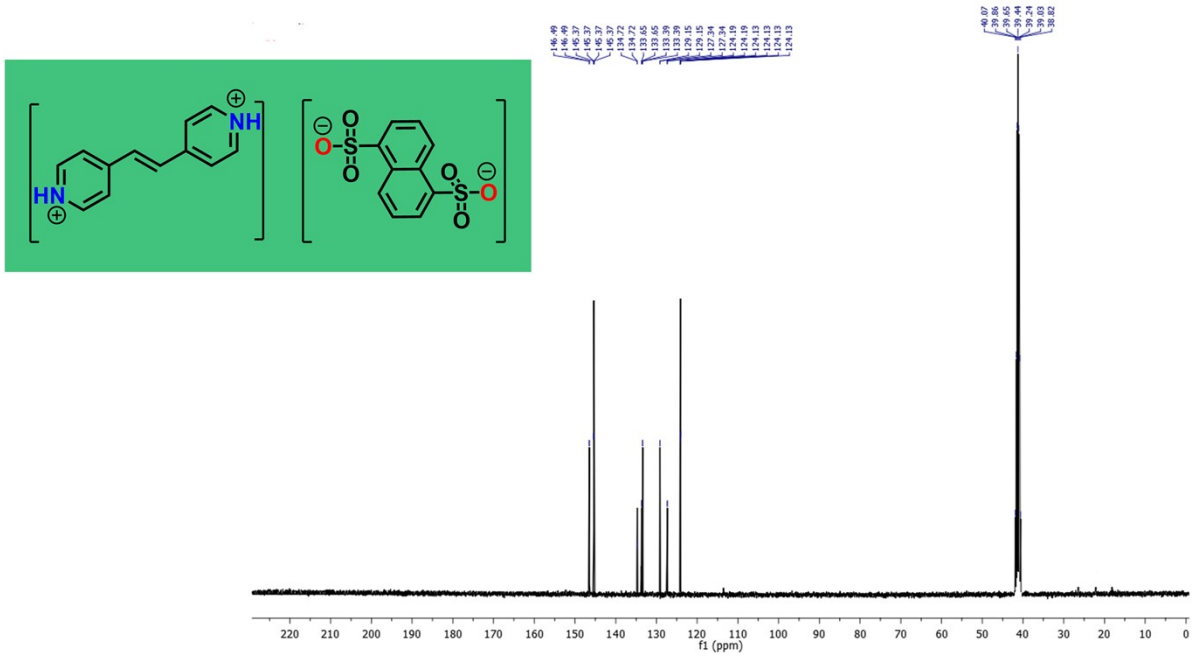

Figure S3: ^{13}C-NMR spectra of **P1** recorded in DMSO-d_6 solvent (500MHz).

^{13}C NMR (500 MHz, DMSO-d_6) δ 146.59 – 146.38 (m), 145.56 – 145.17 (m), 134.91 – 134.52 (m), 133.75 – 133.54 (m), 133.49 – 133.28 (m), 129.25 – 129.04 (m), 127.44 – 127.23 (m), 124.30 – 123.93 (m).

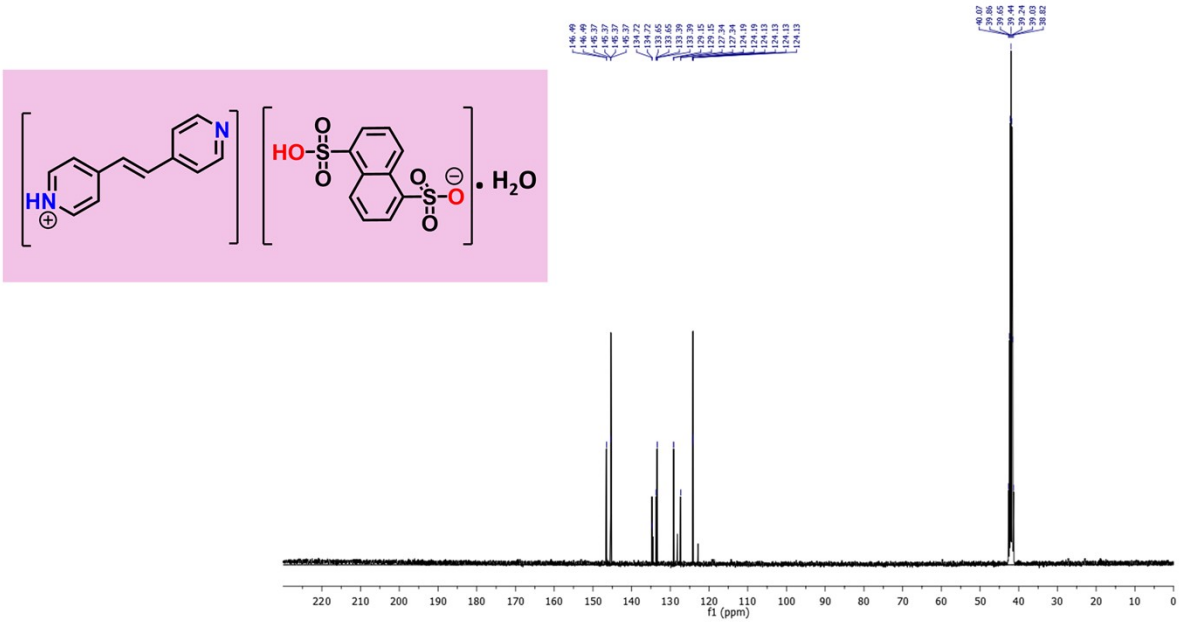

Figure S4: ^{13}C-NMR spectra of **P2** recorded in DMSO-d_6 solvent (500MHz).

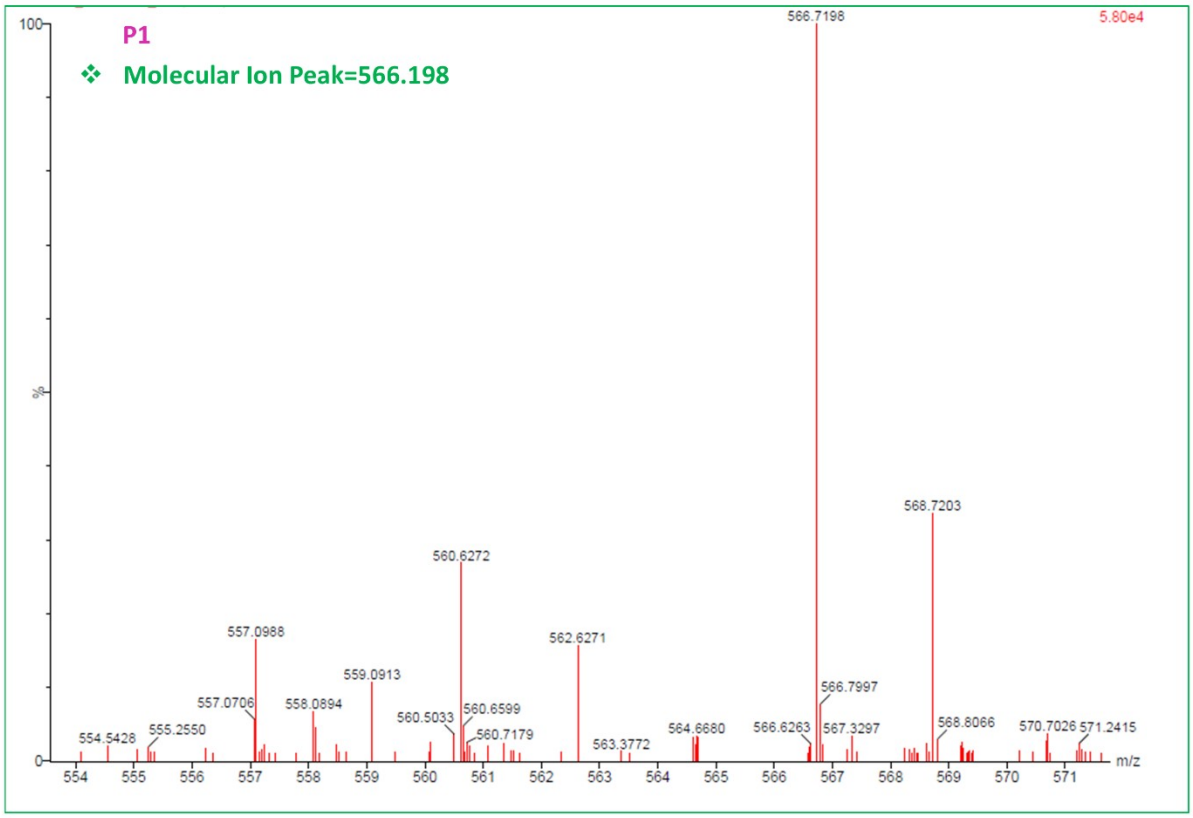

Figure S5: HR-MS Spectra of **P1.**

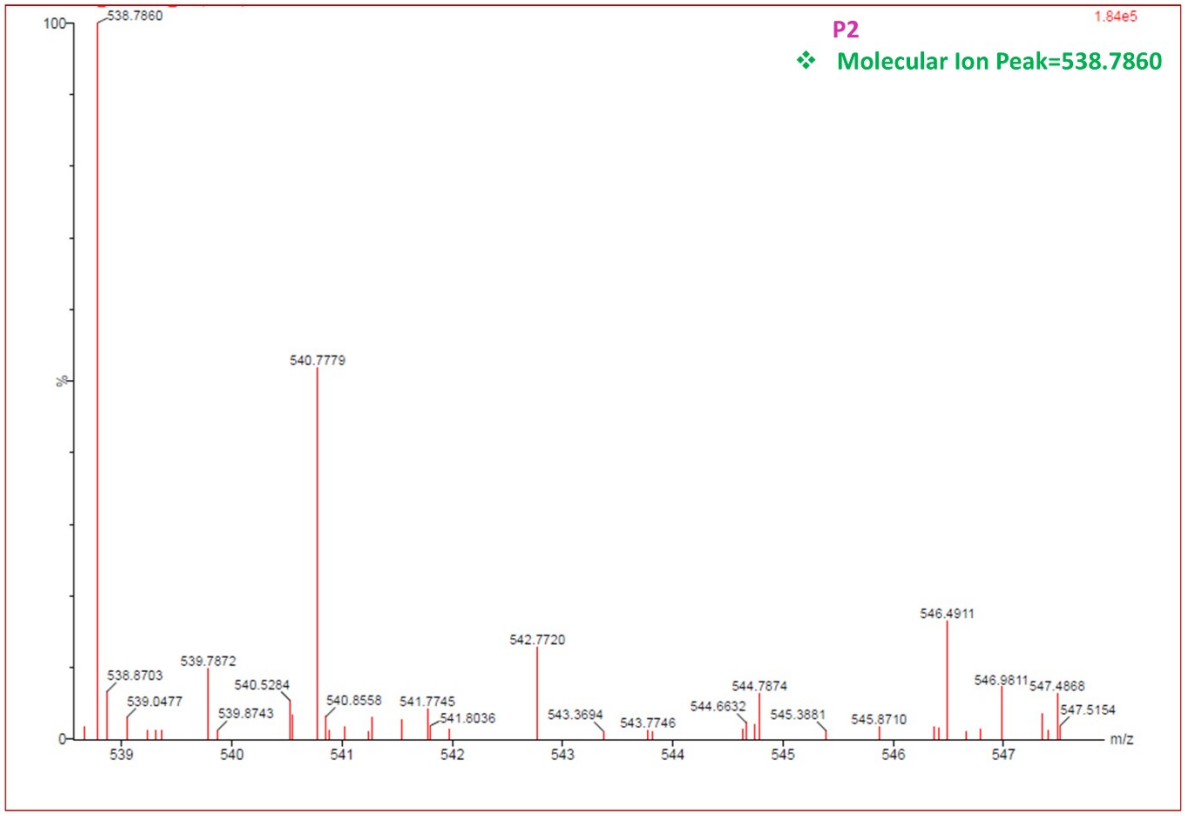

Figure S6: HR-MS Spectra of **P2.**

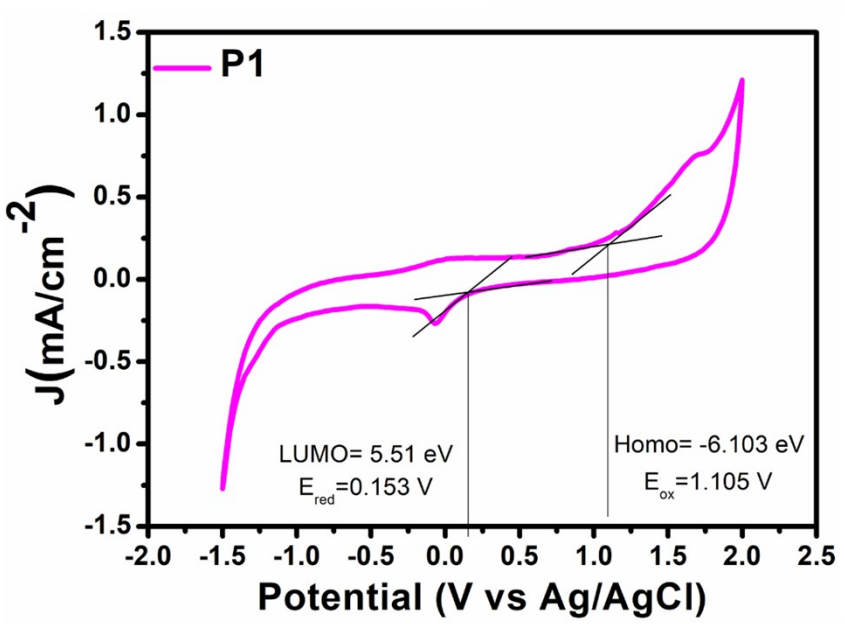

Figure S7: Cyclic Voltammograms of **P1** and calculated HOMO-LUMO gaps.

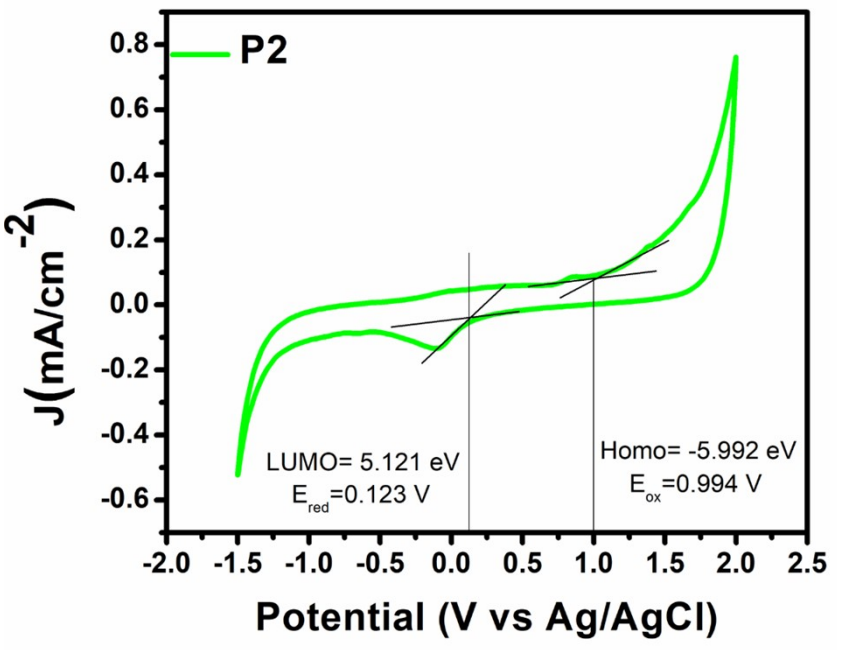

Figure S8: Cyclic Voltammograms of **P2** and calculated HOMO-LUMO gaps.

Table S2: Comparative λ_{abs} (nm), λ_{em} (nm), τ_{avg} (ns), and PLQY values of **P1** and **P2**.

Crystal Forms	λ_{abs} (nm)	λ_{em} (nm)	τ_{avg} (ns)	Φ_{PL}
P1	272	490	13.68	31.3 %
P2	289	545	5.26	24.1 %

λ_{abs} is the absorption maxima, λ_{em} is the emission maxima, τ_{avg} is the average lifetime, and Φ_{PL} is the total photoluminescence quantum yield

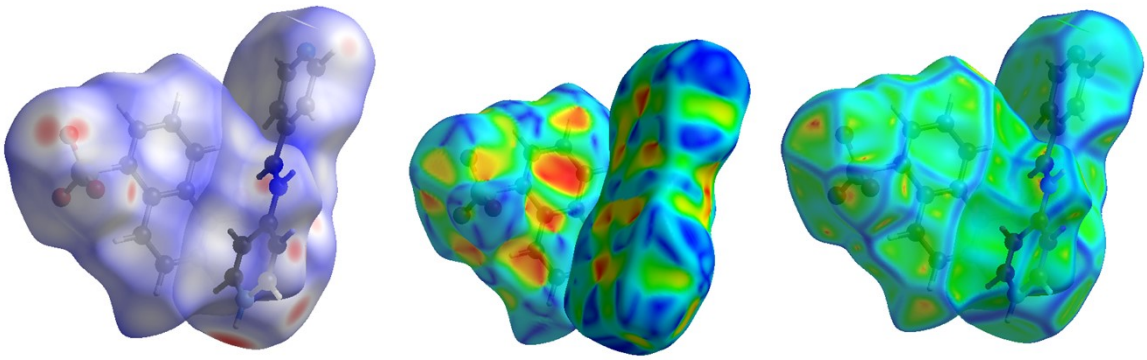

Figure S9: d_{norm}, Shape-index, and Curvedness surface of molecular solid **P1**.

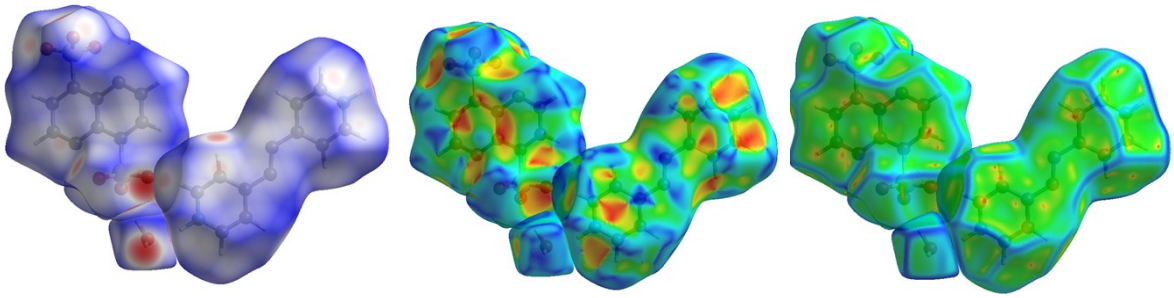

Figure S10: d_{norm}, Shape-index, and Curvedness surface of molecular solid **P2**.

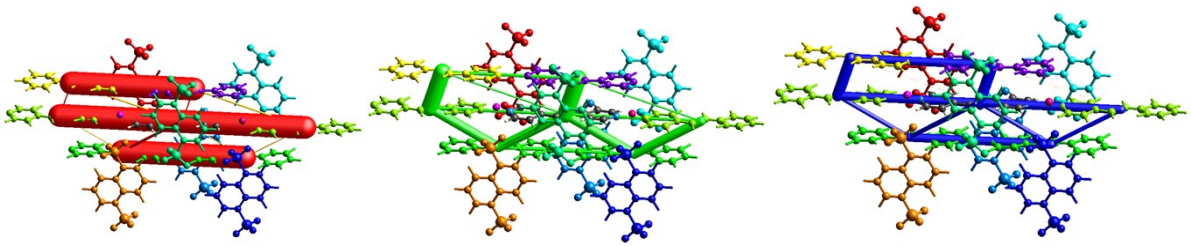

Figure S11: Columb energy, dispersion energy, and total energy calculations of **P1.**

.

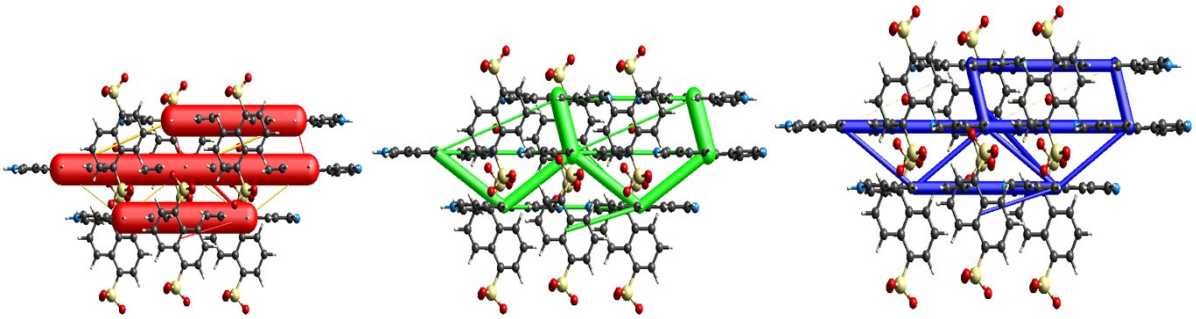

Figure S12: Columb energy, dispersion energy, and total energy calculations of **P2.**

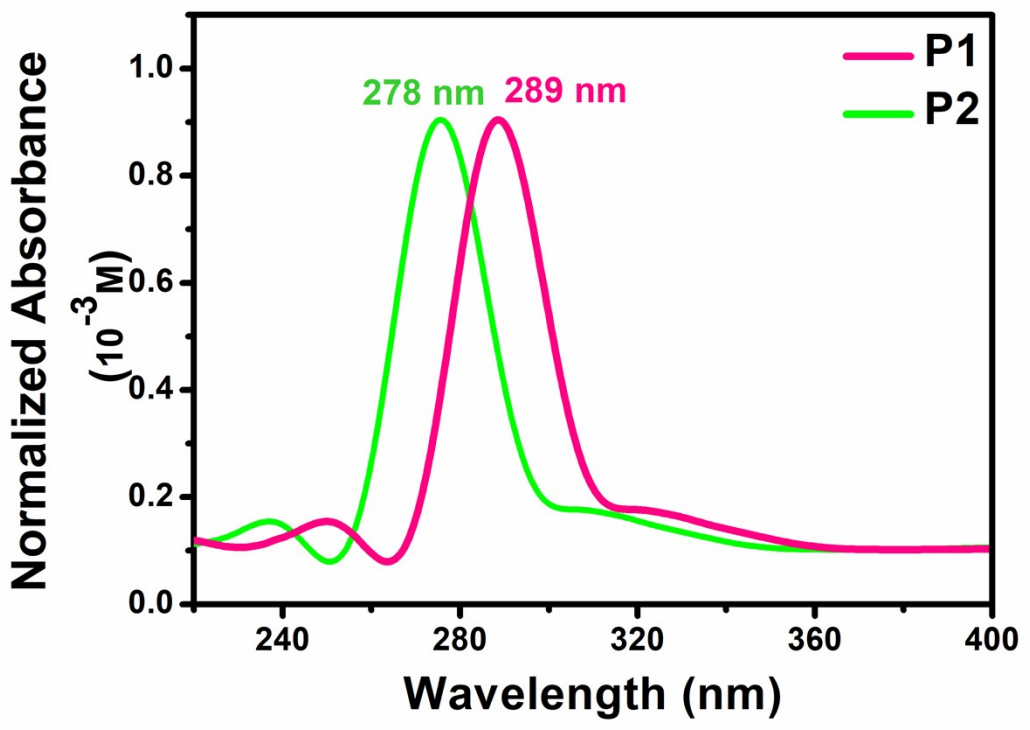

Figure S13: Absorption spectra (normalized to 1) of **P1** and **P2** in THF(10^{-3} M conc.).

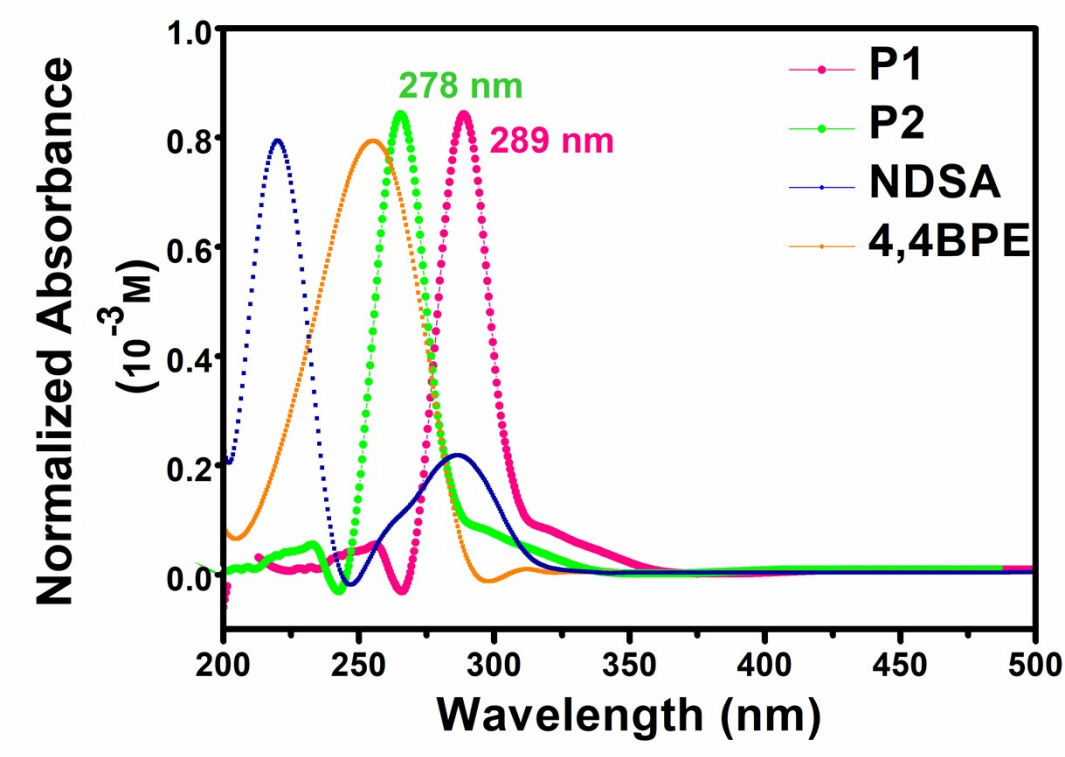

Figure S14: Absorption spectra (normalized to 1) of **P1** and **P2** compared with the precursors in THF (10^{-3} M conc.).

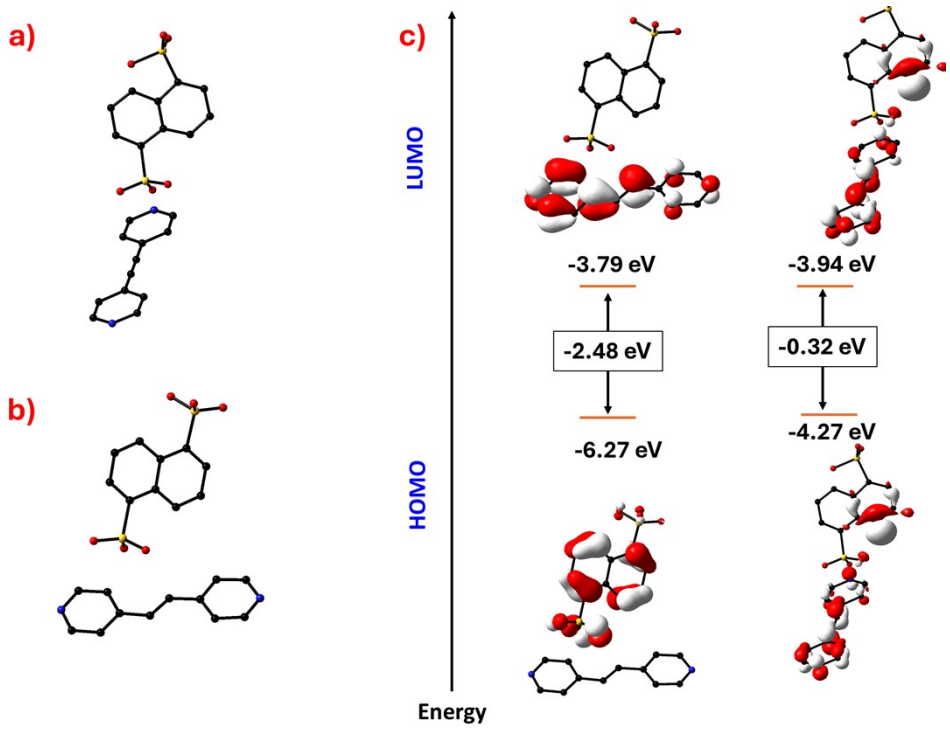

Figure S15: Ground state (S_0) optimized geometry of compounds (a) **P1**, and (b) **P2**. (c) Frontier molecular orbital diagram (iso value 0.04) and corresponding energy values for **P1** and **P2**. The theoretical calculations are performed using density functional theory (DFT) at the B3LYP/6-31G(d) level of theory by taking the coordinated form molecular structure obtained from single crystal XRD.

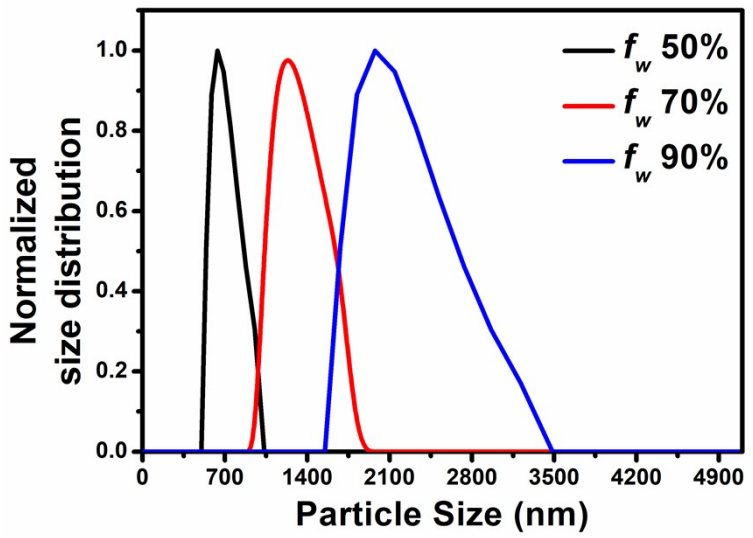

Figure S16 (a) : Dynamic Light Scattering (DLS) Size Distribution Profiles of AIE **P1**.

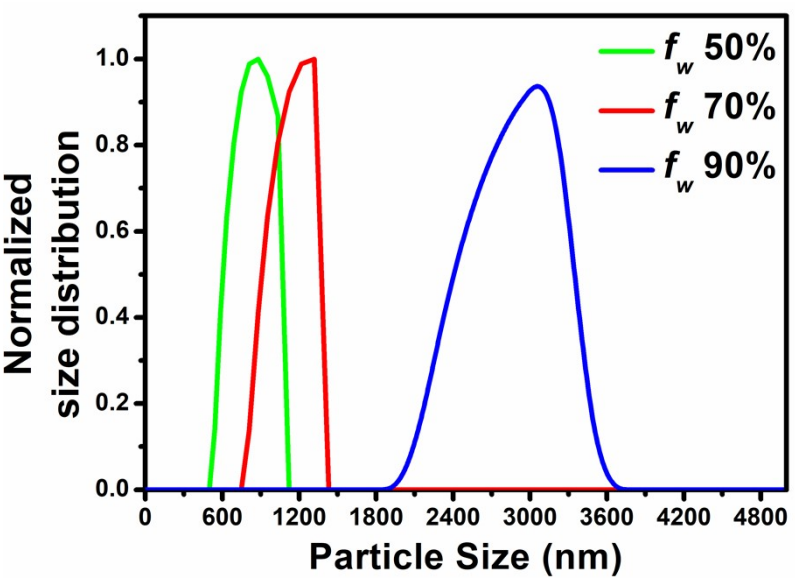

Figure S16 (b) Dynamic Light Scattering (DLS) Size Distribution Profiles of AIE **P2**.

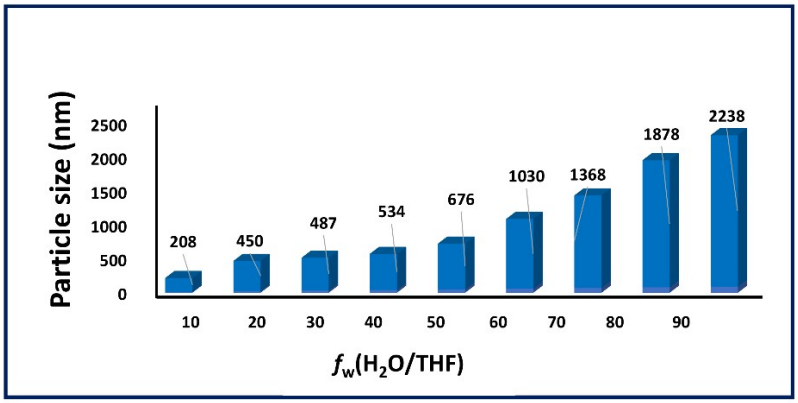

Figure S17 (a) : DLS studies of **P1**.

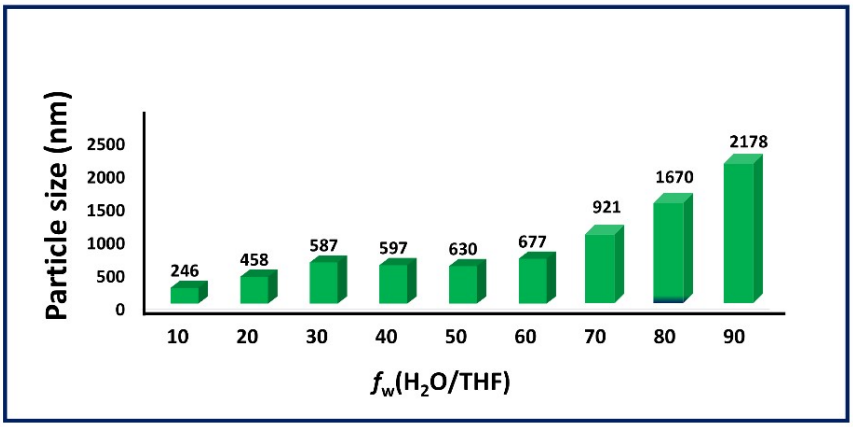

Figure S17 (b): DLS studies of **P2**.

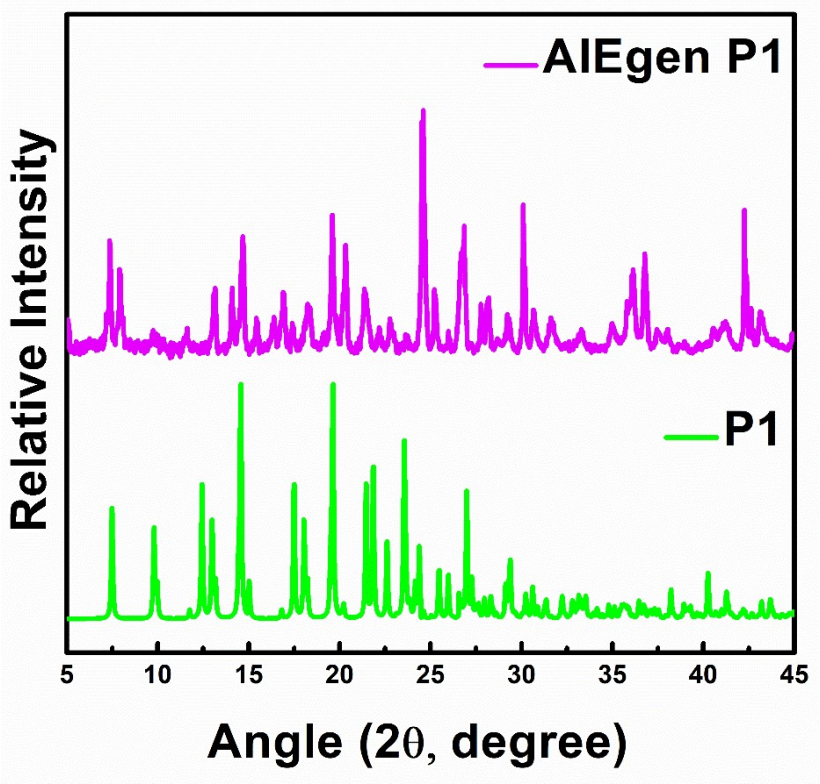

Figure S18: P-XRD of **P1 as** pristine compared with **AIEgen P1** (f_w 90 %).

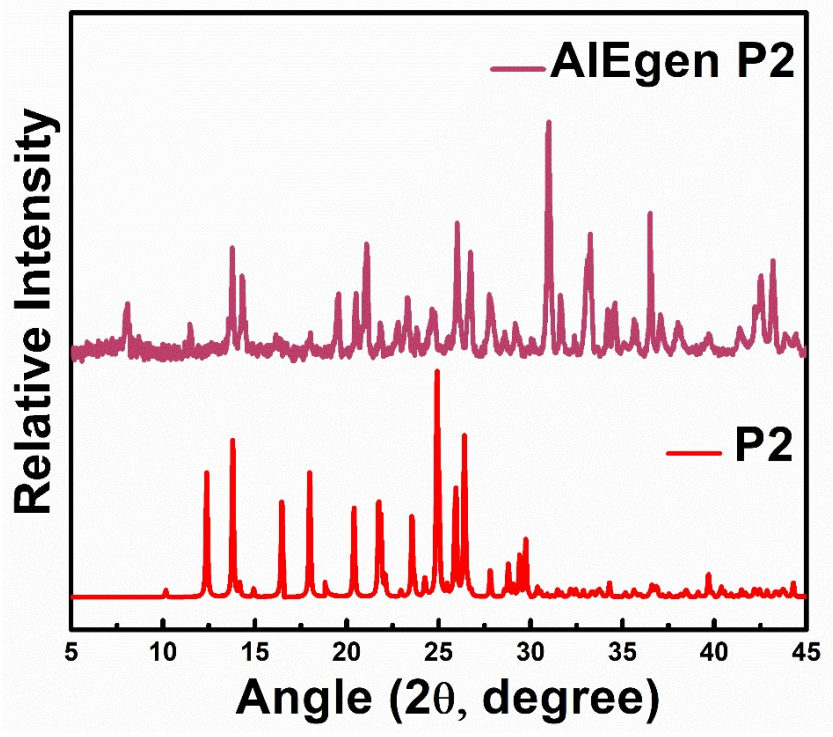

Figure S19: P-XRD of **P2** as pristine compared with **AIEgen P2** (f_w 90 %).

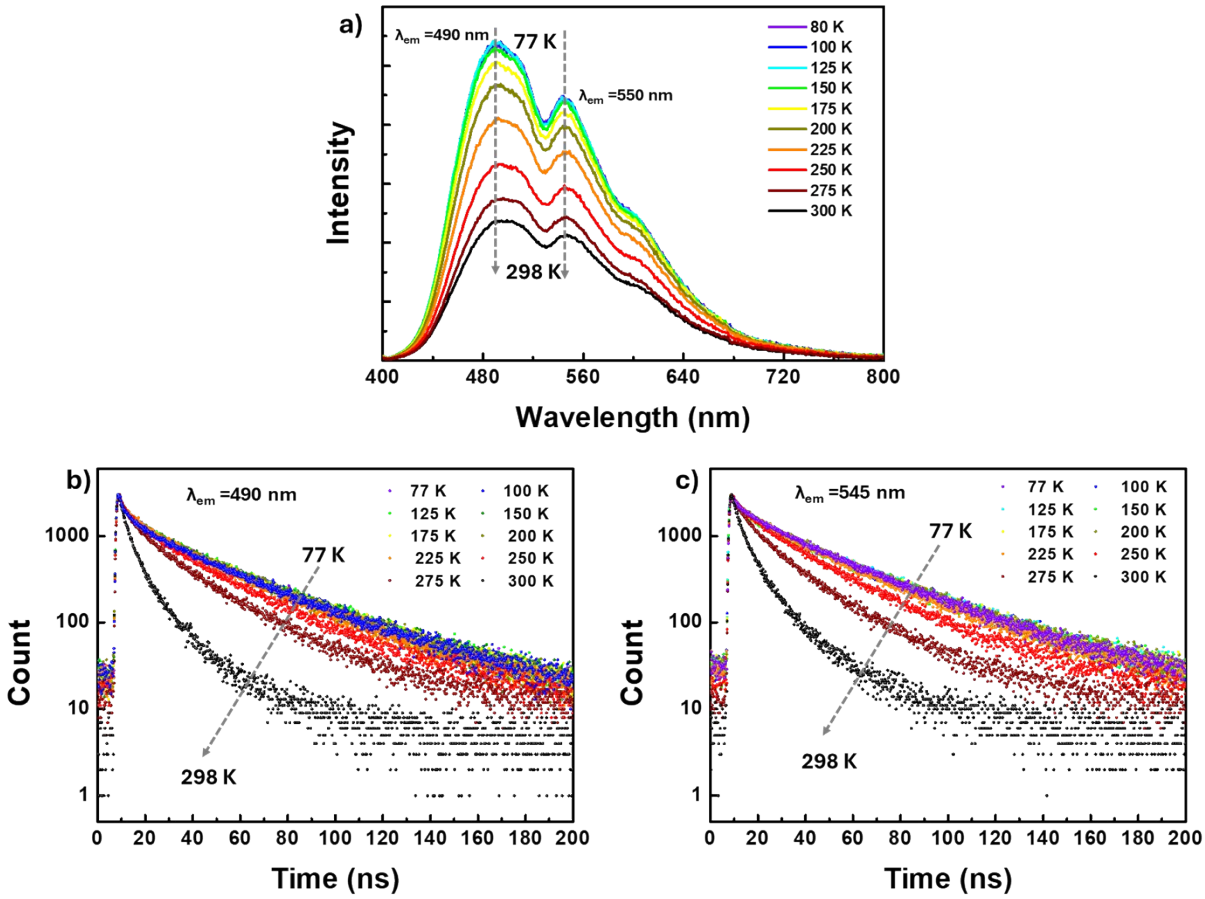

Figure 20: (a) Steady-state photoluminescence Spectra at λ_{ex} = 375 nm and (b,c) fluorescence decay profiles for the pristine sample of **P1** at different temperatures (b) λ_{ex} = 375 nm λ_{em} = 490 nm and (c) λ_{ex} = 375 nm λ_{em} = 545 nm.

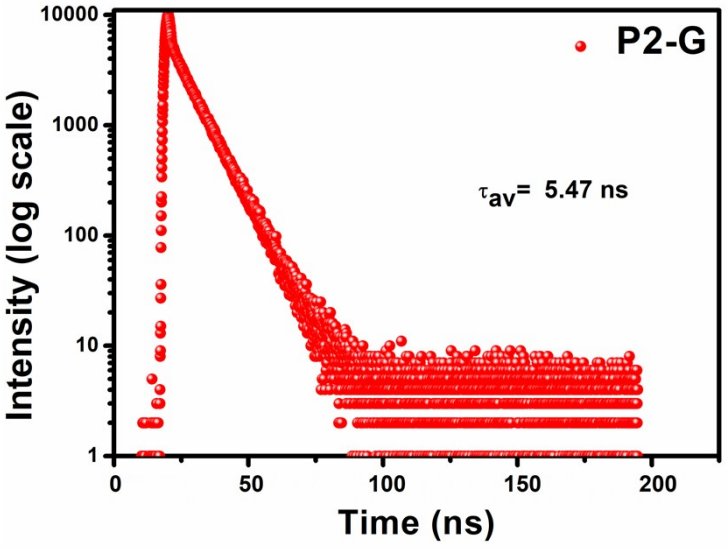

Figure S21: Fluorescence lifetime decay profile of **P2-G** at λ_{ex} = 354 nm, pls put λ_{em} = 545 nm.

Table S3: Lifetime values of the pristine sample of **P1** at different temperatures monitored at λ_{em} = 490 and 545 nm and λ_{ex} = 375 nm .

Temperature (K)	490			545		
	τ_1 [ns] A_1 (%)	τ_2 [ns] A_2 (%)	τ_{av} [ns]	τ_1 [ns] A_1 (%)	τ_2 [ns] A_2 (%)	τ_{av} [ns]
77	6.05 ± 0.21 ns (9.36%)	37.55 ± 0.23 ns (90.64%)	34.60	9.27 ± 0.46 ns (9.27%)	40.43 ± 0.37 ns (90.73%)	37.54
100	6.67 ± 0.21 ns (10.98%)	37.60 ± 0.26 ns (89.02%)	34.20	8.71 ± 0.44 ns (8.46%)	39.76 ± 0.33 ns (91.54%)	37.13
125	6.28 ± 0.20 ns (10.43%)	37.36 ± 0.25 ns (89.57%)	34.11	7.18 ± 0.32 ns (7.57%)	38.89 ± 0.26 ns (92.43%)	36.49
150	5.45 ± 0.17 ns (9.79%)	36.98 ± 0.22 ns (90.21%)	33.89	8.05 ± 0.36 ns (8.61%)	39.09 ± 0.30 ns (91.39%)	36.41
175	5.76 ± 0.19 ns (9.78%)	36.44 ± 0.23 ns (90.22%)	33.44	6.93 ± 0.32 ns (7.25%)	38.08 ± 0.25 ns (92.75%)	35.82
200	6.01 ± 0.19 ns (10.16%)	36.16 ± 0.23 ns (89.84%)	33.09	8.80 ± 0.46 ns (8.46%)	37.68 ± 0.30 ns (91.54%)	35.23
225	6.6 ± 0.21 ns (11.07%)	36.31 ± 0.24 ns (88.93%)	33.02	9.13 ± 0.46 ns (8.88%)	38.00 ± 0.32 ns (91.12%)	35.44
250	6.37 ± 0.20 ns (11.78%)	33.92 ± 0.22 ns (88.22%)	30.67	10.54 ± 0.50 ns (12.51%)	36.54 ± 0.38 ns (87.49%)	33.28
275	7.29 ± 0.25 ns (14.56%)	31.24 ± 0.25 ns (85.44%)	27.75	9.40 ± 0.36 ns (16.39%)	31.57 ± 0.32 ns (83.61%)	27.94
298 ambi	4.68 ± 0.07 ns (49.90%)	21.78 ± 0.32 ns (50.10%)	13.25	4.98 ± 0.07 ns (51.57%)	22.76 ± 0.36 ns (48.43%)	13.60
300	4.5 ± 0.06 ns (58.40%)	18.51 ± 0.32 ns (41.60%)	10.32	5.27 ± 0.07 ns (58.40%)	20.04 ± 0.36 ns (41.60%)	11.41

Table S4: Interaction and lattice energy (kJ/mol) calculation of **P1.**

	N	Symop	R	Electron Density	E_ele	E_pol	E_dis	E_rep	E_tot
	1	-x, -y, z	7.12	HF/3-21G	11.2	-8.1	-19.9	12.0	-2.1
	1	-	8.59	HF/3-21G	-6.1	-5.2	-11.3	10.5	-11.2
	1	-x, -y, z	10.94	HF/3-21G	6.9	-1.7	-7.0	1.1	0.5
	2	x, y, z	11.99	HF/3-21G	-87.3	-31.0	-12.7	112.3	-29.6
	2	-x+1/2, y+1/2, z	6.89	HF/3-21G	3.5	-3.8	-37.1	21.7	-14.9
	1	-	4.92	HF/3-21G	12.7	-17.9	-35.2	22.7	-12.0
	1	-	8.36	HF/3-21G	-4.1	-12.8	-14.8	20.5	-9.3
	1	-	6.89	HF/3-21G	-13.9	-9.0	-14.9	10.8	-24.6
	1	-	9.63	HF/3-21G	-10.5	-3.1	-4.8	2.0	-15.3
	1	-x, -y, z	3.76	HF/3-21G	-4.6	-5.7	-65.8	36.4	-38.1
	1	-	6.41	HF/3-21G	1.6	-1.9	2.0	0.4	-1.7
	1	-	7.76	HF/3-21G	0.6	1.4	0.6	0.8	2.1

Table S5: Interaction and lattice energy (kJ/mol) calculation of **P2.**

	N	Symop	R	Electron Density	E_ele	E_pol	E_dis	E_rep	E_tot
	1	-	7.12	HF/3-21G	11.2	-8.1	-19.9	12.0	-2.1
	1	-	8.59	HF/3-21G	-6.1	-5.2	-11.3	10.5	-11.2
	1	-x, -y, z	10.94	HF/3-21G	6.9	-1.7	-7.0	1.1	0.5
	2	x, y, z	11.99	HF/3-21G	-87.3	-31.0	-12.7	112.3	-29.6
	2	-x+1/2, y+1/2, z	6.89	HF/3-21G	3.5	-3.8	-37.1	21.7	-14.9
	1	-	4.92	HF/3-21G	12.7	-17.9	-35.2	22.7	-12.0
	1	-	8.36	HF/3-21G	-4.1	-12.8	-14.8	20.5	-9.3